

## Polyfluorene derivatives as a promising candidate for coating application

Imen Mechergui<sup>1\*</sup>, Francesco Piana<sup>2</sup>, Miroslav Kohl<sup>1</sup>,  
and Andréa Kalendová<sup>1</sup>

<sup>1</sup> *Institute of Chemistry and Technology of Macromolecular Materials,  
The University of Pardubice, CZ–532 10 Pardubice, Czech Republic*

<sup>2</sup> *Institute of Macromolecular Chemistry, Academy of Sciences  
of the Czech Republic, CZ–162 06 Prague 6, Czech Republic*

Received: April 24, 2023; Accepted: June 27, 2023

*This paper is focused on the synthesis and the characterization of one of the cationic water-soluble conjugated polymers based on polyfluorene (PF) derivatives with terminal amino-groups named poly(9,9-bis(2-(N-ethan(pyrolin-1-yl))ethan)fluorene dibromide (shortly abbreviated as "para phenyl") synthesized by Suzuki-Miyaura coupling reaction and quaternized through a bromoalkylation on pyrrolidine groups, giving rise to a conjugated ammonium polyelectrolyte (P2). The structure of the obtained polyfluorene derivatives (P1 and P2) was confirmed by <sup>1</sup>H NMR and FTIR and their photophysical, electrical, and electrochemical properties fully investigated. The results show that the new polyfluorene electrolyte could be a strong candidate as a coating material thanks to its chemical stability and high conductivity.*

**Keywords:** Polyfluorene derivative; Optical properties; Energy levels; Conductivity; Polymeric coating; Corrosion protection

### Introduction

The past several years witnessed great progress in the use of polymeric materials as a protective coating [1]. In fact, regarding polymers, we start talking about ‘green coating application’ as these materials are replacing heavy metals like chromium and cadmium coatings with harmful effects on the environment [2–4].

---

\* Corresponding author, ✉ imenmechergui20@gmail.com

Such polymers have shown to be effective and proven themselves as a potential alternative for controversial heavy metal coatings in order to control the corrosion properties of metals or alloys. Among them, conducting polymers (CP), such as polyaniline (PANI), polypyrrole (PPY) or polythiophene (PT), have, since their discovery in 1977, opened up new possibilities in their use, having shown significant results in terms of coatings and offering a wide range of applications in the surface engineering [5,6]. Besides the most investigated CPs, polyfluorene derivatives (Pfds) could be also exploited for this field.

It can be stated that, after more than 20 years of progress, these unusual polymers showed tremendous potential for innovation. As an important class of photoactive and electroactive materials, they have been intensively studied during the last few decades by many authors (see e.g. [1,7,8]). Owing to their peculiar advantages of tunable colours, low cost, and easy fabrication, as well as their unique photophysical and electrical properties, they are powerful candidates for anticorrosion materials [8,9]. Moreover, they have already demonstrated good chemical stability and mechanical resistance which are the main weakness of mostly used organic materials in such coating applications [10].

This study highlights the optical and electrochemical activities of our synthesized conducting polyfluorene derivatives, thus representing a good prerequisite for polymeric coating applications, and the way of how they could be promising alternatives to the polymers being hitherto used for these applications, such as PANI and PPy.

## **Experimental**

### **Materials**

All manipulations involving air-sensitive processes were performed under an atmosphere of dry nitrogen. Dimethylformamide (DMF) and tetrahydrofuran (THF) were purified by distillation. All other reagents and solvents were purchased from Merck, Darmstadt, Germany), with the exception of PFN-Br, which was supplied by Sigma Aldrich (St. Louis, MO, USA) and used in analytical grade without further purification.

<sup>1</sup>H-NMR spectroscopy of the synthesised products was performed using an AVANCE-III 600 US+ (Bruker, Billerica, MA, USA). A Paragon 1000 PC Fourier Transform Infrared Spectrometer (Perkin-Elmer, Waltham, MA, USA) was used for FTIR measurement in the KBr pellet.

UV-Vis spectra were recorded with a Lambda 950 Uv/Vis spectrometer (Perkin-Elmer). Fluorescence measurement was carried out on a LS 50B photoluminescence spectrometer (Perkin-Elmer) with a Xe-lamp as a light source. Measurements in the I/V mode were done using a Keithely electrometer.

Cyclic voltammetry (CV) was performed using a potentiostat-galvanostat (model "Amel 7050", Amel electrochemistry, Milano, Italy) connected with a three-electrode cell, where Pt-wire electrodes were used as counter and working electrodes, while Ag/AgCl served as the reference electrode (Amel electrochemistry). CV measurements were made in a solution of 0.1M tetrabutylammonium bromide.

## Synthesis

The polymers were prepared according to the reaction scheme in Figure 1:

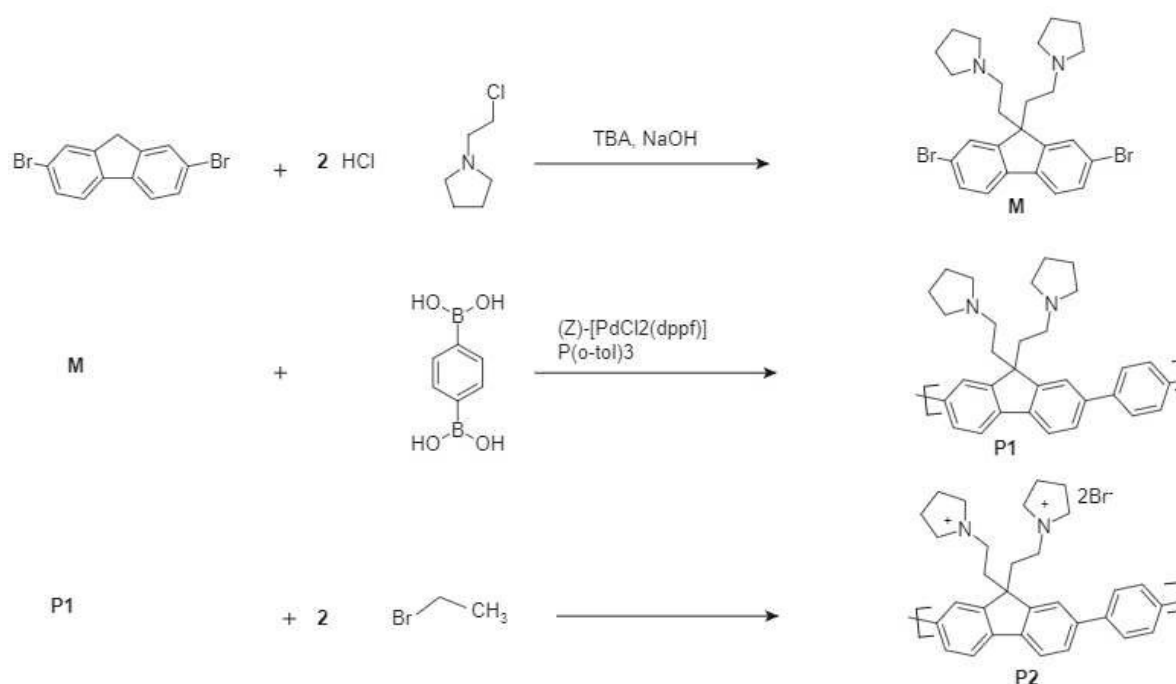


**Fig. 1** The synthetic routes for the monomer and the polymers

The dibromide monomer (M) was synthesized from the reaction of 2,7-dibromofluorene (R1) with two equivalents of 1-(2-chloroethyl)pyrrolidine hydrochloride (R2) in a two-phase mixture of DMSO/H<sub>2</sub>O in the presence of excess NaOH and tetrabutylammonium bromide (TBA) as a phase transfer catalyst. The crude reaction mixture was purified by column chromatography with hexane to give the monomer M (in a yield of 74 %) as a yellowish solid. The Suzuki-Miyaura coupling reaction of the latter with benzene-1,4-diboronic acid (R3) was carried out to obtain the neutral conjugated polymer P1, which was prepared in a mixture of DMF and trimethylamine (4:1) in the presence of tris(*o*-tolyl)phosphine (P(*o*-tol)<sub>3</sub>), catalysed by dichloro[1,1'-bis(diphenylphosphine)ferrocene] palladium(II) ((Z)-[PdCl<sub>2</sub>(dppf)]).

The polymer was finally converted into a brownish polyelectrolyte (P2) by reaction with 5 ml of bromoethane per 100  $\mu\text{g}$  of P1 in 25 ml of THF solution at room temperature for 5–6 days under stirring (with a yield of 83 %).

The resulting neutral polymer P1 was dissolved in common organic solvents, such as THF, DMF, chloroform, and benzene (but it was insoluble in DMSO). After quaternization, the resulting polymer P2 showed complete solubility in DMF, THF, chloroform, methanol, and water, but was insoluble in benzene.

### Sample preparation

Fused silica substrates were used to drop-cast the polymers after dissolution in benzene, THF, and DMF for optical studies and CV. The solutions of both P2 and PFN-Br were filtered with Millex-FH13 Millipore syringe filters (0.45  $\mu\text{m}$ ).

For I/V measurements, ITO-coated glass substrates were used, being first sonicated in detergent, DI water, acetone, and isopropanol, respectively, and then dried in an oven at 90 °C before use. Both polymers, P2 and PFN-Br, were drop-casted onto these ITO substrates after being cleaned by an argon plasma treatment for 10 min to obtain a film thickness of approximately 20 nm. This was measured using a KLA-Tencor P-10 profilometer.

## Results and discussion

### FTIR analysis

The structure of the neutral polymer P1 was confirmed by both  $^1\text{H}$  NMR and FTIR. In particular, the FTIR spectra (see Figure 2) showed characteristic absorption bands for M and P1 appearing between a wavenumber from 2900 to 3000  $\text{cm}^{-1}$ , typical for the presence of stretching vibration bands for aliphatic C-H deformations. The absorption intensity at 1607  $\text{cm}^{-1}$  corresponded to C-C stretching vibration in the aromatic ring (in the fluorene and phenyl ring units). The bands found in a region of 900–700  $\text{cm}^{-1}$  are due to the out-of-plane bending aromatic C-H bonds. The band at 1267  $\text{cm}^{-1}$  originates from C-N group vibration in pyrrolidine ring, when the same interpretation has been reported by Mikroyannidis et al [10].

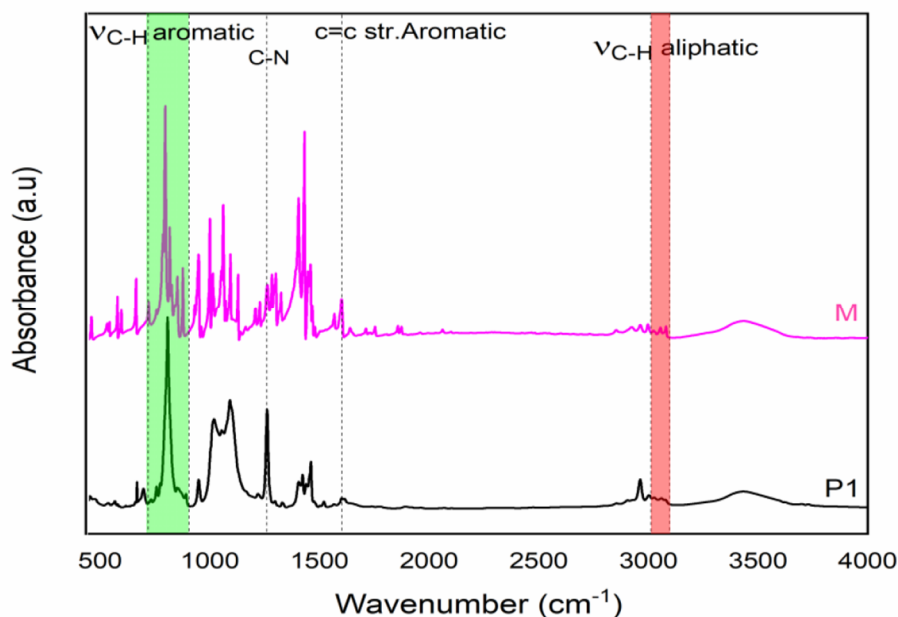


**Fig. 2** FTIR spectra of polymer P1 with monomer M and different reagents

### Photophysical properties

Pendant quaternization is particularly attractive example of a possibility of how to develop new materials that — in addition to their intrinsic polymer backbone chain electronic exploitation — may offer specific properties, which is also the case of our polyfluorene-based cationic synthesized polymer P2.

In the next part, photophysical properties of the self-synthesized polymer P2 were compared to those of a commercial polyfluorene derivative (9,9-bis(3'-(*N,N*-dimethyl)-*N*-ethyl ammoniumpropyl-2,7-fluorene)-alt-2,7-(9,9-dioctylfluorene)) dibromide shortly abbreviated as PFN<sup>+</sup>-Br<sup>-</sup> (Figure 3).

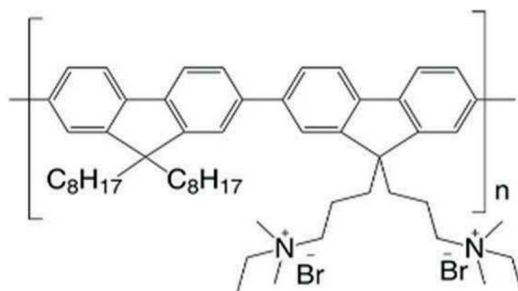


**Fig. 3** Structure of PFN<sup>+</sup>-Br<sup>-</sup>

### UV-Vis absorption

The respective spectra of polymers displayed in Figure 4 demonstrate a strong absorption in the UV-Vis region due to the delocalized structure of PFds [9].

The neutral polymer P1 was dissolved in benzene as well as in DMF, while the polymer P2 was dissolved in DMF at two different concentrations C1 and C2 ( $C1 = 0.5$ ;  $C2 = 2$  mg/1 mL), and coated onto ITO film.

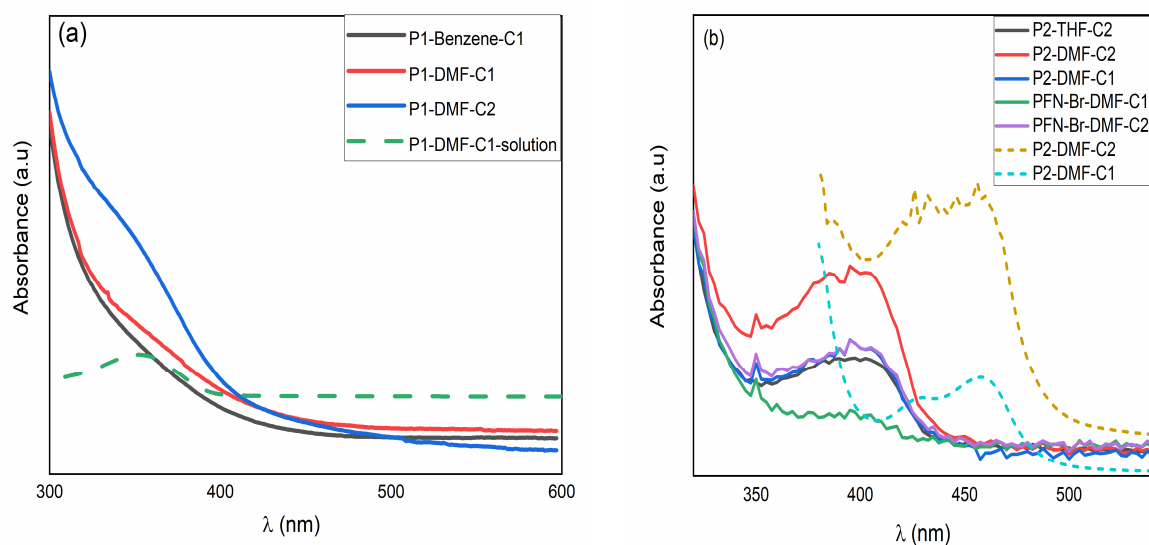


**Fig. 4** UV-Vis absorption of (a) neutral polymer P1 (b) quaternized salt P2 compared to the commercial salt  $\text{PFN}^+\text{-Br}^-$

For neutral polymer P1, its absorption edges for thin films are similar to those in DMF solution (dashed lines) and there is not a clear difference between the curves of P1 dissolved in benzene or DMF. The lowest energy absorption maxima corresponding to the absorption of the  $\pi$ - $\pi^*$  conjugated backbone in P1 were located at around 358 nm and clearly observed in solution compared with those in films the same results were observed in previous work about polyfluorene derivatives with triphenylamine [11].

The thin film UV-vis absorption spectra of the synthesized salt P2 are displayed in Figure 4-b and compared to those in solution as well as those of the commercial salt  $\text{PFN}^+\text{-Br}^-$ .

The onset of the absorption in P2 and PFN-Br thin films was at around 400 nm while the absorption spectra of P2 in the solution redshifted with a maximum at around 460 nm, indicating a strong aggregation when being in the solution state. At the molecular level, conjugated polymers are known to consist of rigid conjugated backbones. However, in the solution, these polymers exhibited a high tendency to aggregate due to the strong molecular interchain interactions [12]. These aggregates would be incorporated into the solid-state microstructure during the film formation process from deposition to drying, which has been shown to affect the morphological and photophysical properties [13,14].

The most well-known basic forms of aggregates are H, and J cumulations and there are other types of unconventional, assembled, and mixed forms [15,16]. Co-facial parallel transistor dipole H aggregates exhibit a blue shift in absorption

spectra and quenching in the emission spectra while J aggregates, resulting in a slipping of molecules along the directions of transition dipoles, generate a very moderate redshift and strong fluorescence in the emission spectra [12].

The polyelectrolyte P2 dissolved in DMF has been found to form  $\pi$ -stacks of H-aggregates in drop-casted films based on the results of UV-Vis absorption measurements where the spectra of the DMF solutions of the polymer P2 were blue-shifted from those of the drop-casted ITO films of the solutions. Similar results were found for some conducting polymers, such as poly(3-hexylthiophene) (P3HT), which is a poly-thiophene derivative, a conductive polymer that is widely used as a material for organic coatings [12]. H-type aggregates are beneficial for charge transport due to the  $\pi$ - $\pi$  overlap that is greatly needed for protective organic coating.

Some works suggested that the nature of the solvent and its solubility can greatly impact the aggregation structure of the polymer [17] but, in our case, this effect is unclear and a further verification of photoluminescence (PL) spectroscopy should be performed when studying more samples with different solvents and concentrations.

The absorption capabilities of P2 and PFN<sup>+</sup>-Br<sup>-</sup> ITO films using different solvents have not been significantly altered, apart from a slight variation in the intensity, indicating that their aggregate state had not been changed [13].

### *Optical energy band gap*

Among the important optical parameters that we can extract from the UV-Vis spectra is the optical energy band gap of the polymers. It was evaluated from the thin-film absorption edge using the Tauc model [18], when assuming that the optical absorption coefficient  $\alpha$  of a semi-conductor is energy ( $h\nu$ ) included in the equation (1):

$$(\alpha h\nu)^{1/n} = C (h\nu - E_g) \quad (1)$$

where  $h$  is Planck constant,  $\nu$  is photon's frequency,  $E_g$  is optical band gap energy,  $C$  is a constant, and  $\alpha$  is the absorption coefficient,  $n$  is a factor that depends on the nature of the electron transition and is numerically equal to 1/2, 3/2, 2, or 3 for direct allowed, direct forbidden, indirect allowed, or indirect forbidden transitions, respectively.

Figure 5 illustrates the variation of  $(\alpha h\nu)^{1/2}$  measured by  $(\text{cm}^{-1} \text{ eV})^{1/2}$  of on the phonon energy  $h\nu$ . The parameter  $E_g$  was then obtained by extrapolating the linear segment of the curve, showing an increase in light absorption. In some materials, there are two gap energies and these phenomena can arise from multiple absorption processes or different types of electronic transitions, which is common in most polyelectrolytes.

The estimated intrinsic  $E_g$  was found to be around 2.7 eV for the synthesized polyelectrolyte P2, corresponding to a blue wavelength absorption and it presents the minimum energy required for an electronic transition occurring in the polymer. The second peak was generated at around 3.5 eV, it is probably attributed to the transitions of non-bonding electrons in dopant atoms in  $sp^2$  and  $sp^3$  matrices. These results were found in good agreement with previously reported results about some polyelectrolytes and polyfluorene derivatives [11,18].

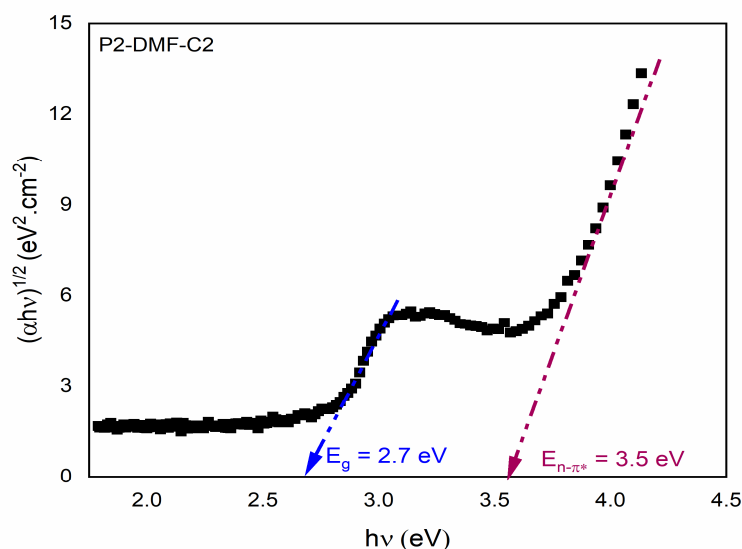


**Fig. 5** Optical energy band gap of quaternized salt P2

### *Photoluminescence properties*

The photoluminescent spectra of the polymer P2-DMF and  $\text{PFN}^+\text{-Br}^-$  films are shown in Figure 6. P2-DMF-C1 and P2-DMF-C2 fluorescence in the orange region at 560 nm and at 570 nm for the commercial polyelectrolyte  $\text{PFN}^+\text{-Br}^-$  when excited by a light source of 400 nm, as already observed in the literature [7–10].

The systematic insight into the relationship between the aggregation structure and the emission property had been thoroughly investigated in many research works [13,14,16], and recently, it has been demonstrated that for organic  $\pi$ -conjugated polymers, the photoluminescence properties can be largely influenced by the aggregation structures. Such cumulations were found to affect not only the emission colour, but also the fluorescence efficiency.

From Figure 6, we notice that the photoluminescence intensity released by the films of the polymer P2 dissolved into DMF with a concentration C1 increased 3.4 times with the two-fold concentration. This result can give us a piece of information about the formation of J aggregates [16].



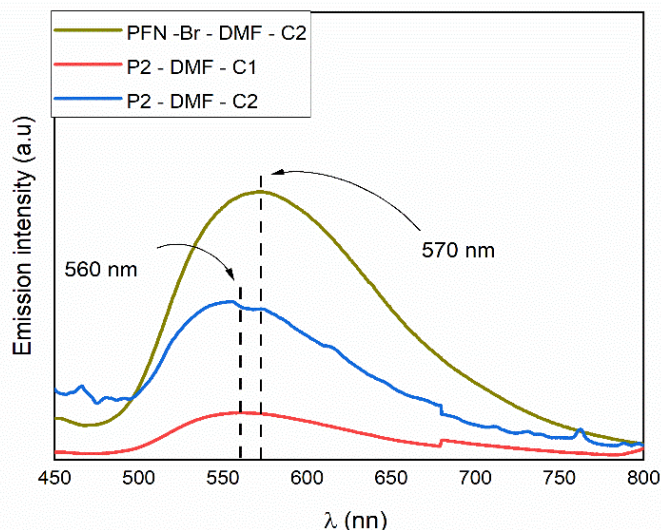


**Fig. 6** Emission spectra of P2 and  $\text{PFN}^+\text{-Br}^-$  thin films under excitation of 400 nm

## Electrical and electrochemical properties

### *Current-voltage measurement (I/V)*

In order to investigate the electrical properties of the synthesized polyelectrolytes, we fabricate OLED (Organic Light Emitting Diodes) devices with the polymers. ITO-coated glass ( $2.5\text{ cm} \times 2.5\text{ cm}$ ) with a resistivity of  $2 \cdot 10^{-4}\ \Omega\text{ cm}$  was etched with HCl in 2 mm strips to define two-hole injection indium tin oxide anodes (ITO). After wet cleaning, the ITO substrates so prepared were cleaned using UV ozone for 10 min., then drop-cast the polymer solution P2-DMF-C2 onto them and annealed at  $60\text{ }^\circ\text{C}$  for 30 min.

Subsequently, three 60-nm thick aluminum (Al) cathodes were deposited by physical vapor deposition (PVC) using a MiniLab 060 thermal evaporator from Moorfield60 thermal evaporator. The single-layer device of ITO/P2/Al is shown in Figure 7.

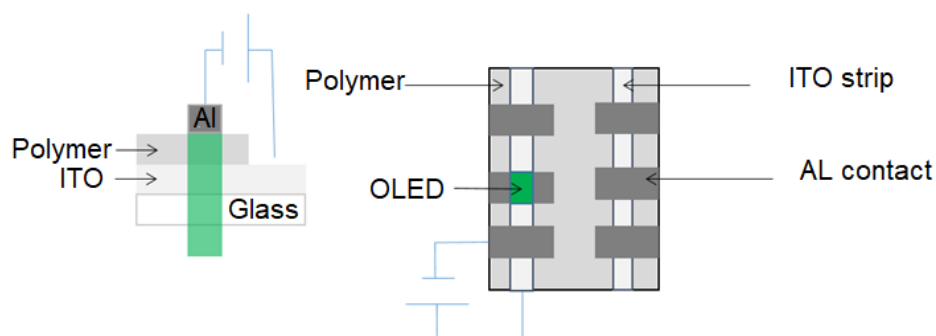


**Fig. 7** The polymer OLED device structure: Side and top views

The current-voltage characteristic of the single-layer OLED of P2-DMF-C2 at room temperature is plotted in Figure 8. It was found that the operating voltage of the device under investigation was  $\approx 0\text{--}8$  V.

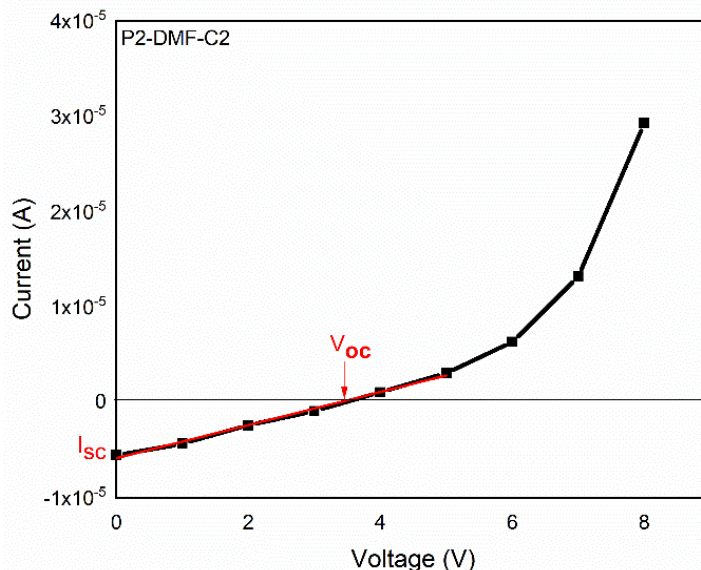


**Fig. 8** I/V characteristic of polymer P2-DMF-C2

To obtain an insight into the conduction mechanism of the device, it was expected the formation of an ohmic contact between the ITO strips and the polymer layer. Therefore, the I/V data were analyzed based on the space charge limited current theory (SCLC).

The transport follows the ohmic behaviour (eq. 2) at low voltage with current density [19]

$$J = q \cdot N \cdot \mu \cdot \frac{V}{d} \quad (2)$$

where  $q$  is the elementary charge,  $N$  is the volume density of charge,  $\mu$  is the carrier mobility, and  $V$  is the applied voltage. When illuminated as in Figure 6, even without the application of an external voltage, a photocurrent occurs which determines the value of the  $I_{sc} \approx -5.7 \cdot 10^{-6}$  A. This photocurrent is reverse current as electrons flow towards the cathode and holes. By applying voltage, a forward bias current begins to compensate for this backward photocurrent until it reaches a point where the current is zero. This voltage corresponds to the open-circuit voltage,  $V_{oc} \approx 3.52$  V, where the system is assumed as open since no current flows under the voltage applied. At higher voltages, the I/V characteristic shows an exponential-like behaviour indicating an increase in the conductance at this range; the same results being found for polyfluorene derivatives [20].

## Electrochemical properties

Cyclic voltammetry was used to study the redox properties of the polymer P2, as well as to estimate the values of the highest occupied molecular orbital (HOMO) and the lowest unoccupied molecular orbital (LUMO) levels. As shown in Figure 9, the oxidation potential,  $E_{\text{ox}}$ , for polymer P2 was found to be 1.22 V vs. ref. and from this value we can estimate the HOMO level of the polymer P2 using the most frequently recommended equation (3, [21]):

$$E_{\text{HOMO}} = -[4.8 + E_{\text{ox}} - E_{1/2\text{Fer}}] \quad (3)$$

where  $E_{1/2\text{Fer}}$  is the half-wave potential of  $\text{Fe}/\text{Fe}^+$  found to be  $-0.6$  V.

The value of the HOMO level of the polyelectrolyte P2 calculated according to (3) was  $-5.42$  eV, thus being similar to that published by Mikroyannidis et al [10]. The LUMO energy level of the polymer P2 could be estimated from the optical energy gap (2.7 eV); then, the parameter  $E_{\text{LUMO}}$  of this polymer was found to be around 2.72 eV. Again, such values are quite close to those obtained for PANI, and PPy [22,23].

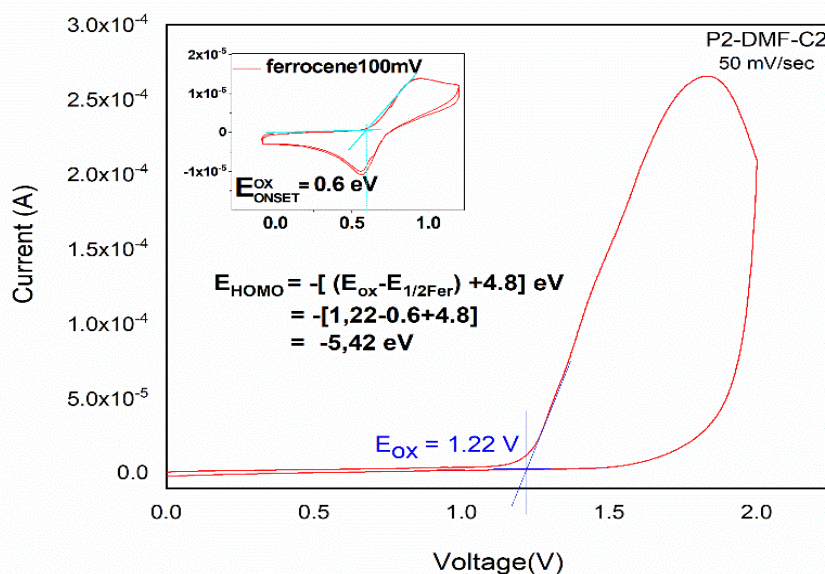


**Fig. 9** Cyclic voltammogram for the polymer P2-DMF-C2

## Conclusions

In summary, structural, photophysical, electrical, and electrochemical characteristics of self-synthesized polyconjugate fluorene derivatives have been measured and compared to a commercial polyfluorene derivative ( $\text{PFN}^+\text{-Br}^-$ ). To test the feasibility of this conducting polymer as a conductive organic layer, Fourier-transform infrared (FTIR) and UV-vis spectroscopy, photoluminescence (PL),

current-voltage measurements (*I-E* curves), and cyclic voltammetry (CV) were performed. Large emission wavelengths originating from PFDs were localized in the range of 560–570 nm, suggesting one an orange PL emission for P2 with maximum at 560 nm. The  $\pi$ -stacks of H-aggregates were formed after drop-casted the P2-DMF solutions onto the ITO films at the two-fold concentration of these solutions, J-aggregates could be formed, which greatly affected the morphology of the prepared films. The HOMO energy level of P2 (5.47 eV) was calculated from the first oxidation peak and LUMO energy level then estimated by optical method from the band gap energy.

The values obtained are quite similar to those of PANI and PPy energy levels, which suggests the possibility of using this kind of polymer for protective coating. We believe that polyfluorene electrolytes are promising conducting materials for organic coating, but their ascertained properties are still challenging and needing to be investigated into more detail, which could result in a significant progress in this field.

## **Acknowledgment**

*The authors would like to thank the UNESCO/IUPAC Postgraduate Course in Polymer Science (year 2021–2022) for financial support by the Institute of Macromolecular Chemistry (IMC) and the Czech Academy of Sciences (CAS), Prague, Czech Republic. All the measurements were performed at the Department of Polymers for Electronics and Photonics of the IMC.*

## **References**

- [1] De Boni L., Fonseca R.D., Cardoso K.R., Grova I., Akcelrud L., Correa D.S., Mendonça C.R.: Characterization of two- and three-photon absorption of polyfluorene derivatives. *Journal of Polymer Science Part B: Polymer Physics* **52** (2014) 747–754.
- [2] Gagaoua M., Bhattacharya T., Lamri M., Oz F., Dib A.L., Oz E., Tomasevic I.: Green coating polymers in meat preservation. *Coatings* **11** (2021) 1379.
- [3] Lan P., Nunez E.E., Polycarpou A.A.: Advanced polymeric coatings and their applications: Green tribology. *Encyclopedia of Renewable and Sustainable Materials* **4** (2020) 345–358.
- [4] Kohl M., Kalendová A., Černošková E., Bláha M., Stejskal J., Erben M.: Corrosion protection by organic coatings containing polyaniline salts prepared by oxidative polymerization. *Journal of Coatings Technology and Research* **14** (2017) 1397–1410.
- [5] Contri G., Zimmermann C.A., Ramoa S.D.A.D.S., Schmitz D.P., Ecco L.G., Barra G.M.O, Fedel M.: (2020) Polypyrrole modified e-coat paint for corrosion protection of aluminum AA1200. *Frontiers in Materials* **7** (2020) 45.

- [6] Ocampo C, Armelin E, Liesa F, Alemán C., Ramis X., Iribarren J.I.: Application of a polythiophene derivative as anticorrosive additive for paints. *Progress in Organic Coatings* **53** (2005) 217–224.
- [7] Liu S.-P., Ng S.-C., Chan H.S.O.: Novel fluorene–pyridine-based alternating copolymers: Synthesis, characterization, and optical properties. *Synthetic Metals* **149** (2005) 1–11.
- [8] Guo F., Zhang M., Zhao S., Hu L., Xiao B., Ying L., Yang R.: Efficient polyfluorene derivatives for blue light-emitting diodes enabled by tuning conjugation length of bulky chromophores. *Dyes and Pigments* **199** (2022) 110059.
- [9] Leclerc M.: Polyfluorenes: Twenty years of progress. *Journal of Polymer Science Part A: Polymer Chemistry* **39** (2001) 2867–2873.
- [10] Mikroyannidis J.A., Barberis V.P., Cimrová V.: Novel electroluminescent cationic polyelectrolyte based on poly[(fluorene-2,7-diylvinylene)-alt-(1,4-phenylenevinylene)] and its precursor. *Journal of Polymer Science Part A: Polymer Chemistry* **45** (2007) 1016–1027.
- [11] Adsetts J.R., Zhang R., Yang L., Chu K.C., Wong J.W.C., Love D.J., Ding Z.: Efficient white electrochemiluminescent emission from carbon quantum dot films. *Frontiers in Chemistry* **8** (2020) 580022.
- [12] Eder T., Stangl T., Gmelch M., Remmerssen K., Laux D., Höger S., Lupton J.M., Vogelsang J.: Switching between H- and J-type electronic coupling in single conjugated polymer aggregates. *Nature Communications* **8** (2017) 1641.
- [13] Gao M., Wang W., Hou J., Ye L.: Control of aggregated structure of photovoltaic polymers for high-efficiency solar cells. *Aggregate* **2** (2021) e46.
- [14] Ding L., Wang Z.-Y., Yao Z.-F., Liu N.-F., Wang X.-Y., Zhou Y.-Y., Luo L., Shen Z., Wang J.-Y., Pei J.: Controllable transformation between the kinetically and thermodynamically stable aggregates in a solution of conjugated polymers. *Macromolecules* **54** (2021). 5815–5824.
- [15] Gu P., Yin Z., Zhao H., Liu Y., Wang W., Ye J., Wang H., Song W.: Performance regulation of perovskite solar cells via bifacial modification by F4-TCNQ and PFN-Br. *Journal of Physical Chemistry C* **126** (2022) 15128–15134.
- [16] Ma S., Du S., Pan G., Dai S., Xu B., Tian W.: Organic molecular aggregates: From aggregation structure to emission property. *Aggregate* **2** (2021) e96.
- [17] Li T., Zhang H., Liu B., Ma T., Lin J., Wang L., Lu D.: Effect of solvent on the solution state of conjugated polymer P7DPF including single-chain to aggregated state structure formation, dynamic evolution, and related mechanisms. *Macromolecules* **53** (2020) 4264–4273.
- [18] Jubu P.R., Obaseki O.S., Nathan-Abutu A., Yam F.K., Yusof Y., Ochang M.B.: Dispensability of the conventional Tauc’s plot for accurate bandgap determination from UV-Vis optical diffuse reflectance data. *Results in Optics* **9** (2022) 100273.
- [19] Peng Q., Lu Z., Huang Y., Xie M., Han S., Peng J., Cao Y.: Synthesis and characterization of new red-emitting polyfluorene derivatives containing electron-deficient 2-pyran-4-ylidene-malononitrile moieties. *Macromolecules* **37**, (2004) 260–266.
- [20] Santos L.P., Gozzi G.: Electrical properties of polymer light-emitting devices. In: Yilmaz F. (Ed.): *Conducting polymers*. InTech eBooks 2016, pp. 145–170.

- [21] Gamini Rajapakse R.M, Watkins D.L., Ranathunge T.A., Malikaramage A.U, Gunarathna H.M.N.P., Sandakelum L., Wylie S., Abewardana P.G.P.R., Egodawele M.G.S.A.M.E.W.D.D.K., Herath W.H.M.R.N.K., Bandara S.V., Strongin D.R., Attanayake N.H., Velauthapillai D., Horrocks B.R.: Implementing the donor-acceptor approach in electronically conducting copolymers *via* electropolymerization. *RSC Advances* **12** (2022) 12089–12115.
- [22] Rangel-Vazquez N.A., Sánchez-López C., Félix F.R.: Spectroscopy analyses of polyurethane/polyaniline IPN using computational simulation (Amber, MM+ and PM3 method). *Polímeros* **24** (2014) 453–463.
- [23] Bilkan Ç.: Determination of structural properties of some important polymers used as interfacial layer in fabrication of Schottky Barrier Diodes (SBDs). *Journal of the Institute of Science and Technology* **10** (2020) 225–233.